CSIRO PUBLISHING

Exploration Geophysics, 2016, **47**, 150–157
http://dx.doi.org/10.1071/EG14110

The 3D inversion of airborne gamma-ray spectrometric data

Brian Minty[1,3] Ross Brodie[2]

[1]Minty Geophysics, PO Box 3229, Weston, ACT 2611, Australia.
[2]Geoscience Australia, GPO Box 378, Canberra, ACT 2601, Australia.
[3]Corresponding author. Email: Brian.Minty@mintygeophysics.com

Abstract. We present a new method for the inversion of airborne gamma-ray spectrometric line data to a regular grid of radioelement concentration estimates on the ground. The method incorporates the height of the aircraft, the 3D terrain within the field of view of the spectrometer, the directional sensitivity of rectangular detectors, and a source model comprising vertical rectangular prisms with the same horizontal dimensions as the required grid cell size. The top of each prism is a plane surface derived from a best-fit plane to the digital elevation model of the earth's surface within each grid cell area.

The method is a significant improvement on current methods, and gives superior interpolation between flight lines. It also eliminates terrain effects that would normally remain in the data after the conventional processing of these data assuming a flat-earth model.

Key words: deconvolution, gamma-ray spectrometry, inversion, terrain correction, topographic correction.

Received 8 November 2014, accepted 26 June 2015, published online 28 July 2015

Introduction

Gamma rays can penetrate up to 30 cm of rock or several hundred metres of air, and are thus suitable for the remote sensing of the radioactivity of the earth using low-flying survey aircraft. The airborne gamma-ray spectrometric method is widely used in mapping applications for both mineral exploration and environmental studies. Gamma radiation measurements are made at airborne survey heights and, through suitable processing, are converted to estimates of the count rates due to the radioelements (K, U and Th) at each observation point along the flight lines. The conventional processing of these data would include a correction for deviations in the aircraft height from the nominal survey height. The elemental count rates are then typically converted to estimates of the elemental concentrations on the ground through a simple scaling of the count rates by a 'sensitivity factor' that depends only on the energy of the primary radiation and the nominal survey height above ground level (IAEA, 2003). Finally, the elemental count rates are interpolated onto regular grids for imaging and interpretation.

The sensitivity correction is applied on a point-by-point basis, despite the fact that the 'field of view' of an airborne detector can be a circle of up to 700 m diameter on the ground, depending on the height of the detector. For a sample interval along lines of 60 m or less, there is significant overlap between successive fields of view. This results in anomalies due to sharp discontinuities in radioelement concentrations on the ground being represented in the final airborne data as smooth transitions. The solution is to invert the airborne data to elemental concentrations on the ground in a rigorous way that accounts for the degradation of the gamma signal with distance from the source, the distribution of radioelement sources in the ground, and the response function of the detector.

Gunn (1978) described a method for the deconvolution of airborne gamma-ray spectrometric count rates to elemental concentrations on the ground. He used a frequency domain representation of the response of an airborne detector to an infinitely thick vertical prism model, and the application of a Wiener filter to deconvolve 2D radiometric profile data. Druker (2012) described a method for the inversion of profile data that incorporates a 2D topography. The advantage of Druker's approach is that some of the corrections (height correction, sensitivity correction, speed of aircraft) are incorporated into the inversion. Also, no smoothing of the data is required as the problem is evenly-determined.

Craig et al. (1999) extended Gunn's frequency domain treatment to the deconvolution (or downward continuation) of gridded radioelement data. They showed that for high quality gridded data, their denoising and deconvolution treatment could produce sharper, more useful, gridded representations of the data. Billings et al. (2003) presented a method for the frequency domain deconvolution of gridded radioelement data using a Wiener filter. They extended the work of Craig et al. to incorporate into their model the directional sensitivity of the rectangular detectors in common use today, and the movement of the detector through the air. The deconvolution effectively corrects for both the nominal survey height and the directional sensitivity of the detector with a view to sharpening up the edges of anomalies.

The methods described by Craig et al. and Billings et al. represent significant advances in the processing of airborne gamma-ray data, and are routinely used for the enhancement of high-quality gridded gamma-ray spectrometric data. However, they are limited in the following respects:

- The methods are for the enhancement of gridded gamma-ray spectrometric data. Typically, minimum curvature or cubic spline interpolation are used to grid the gamma-ray line data. But these methods are not well suited to gamma-ray spectrometric data, as they tend to smooth the edges of radioelement anomalies in the first place.
- The methods use a flat-earth model. In reality, undulating topography has a significant effect on the gamma-ray response. For example, as the aircraft goes over the top of a hill, sources directly beneath the aircraft have a significantly greater contribution to the observed gamma-ray fluence rate

than would be the case if the earth was flat. The opposite is true when the aircraft traverses a valley. Also, in rugged topography, some areas of the earth's surface that would nominally be within the field of view of the detector (if the earth were flat) may be hidden from view by the topography.

The solution is to invert the gamma-ray spectrometric line data directly to a regular grid of radioelement concentrations on the ground using a model that incorporates variations in the topography.

We present a new method for inverting airborne gamma-ray spectrometric line data to a rectangular grid of radioelement concentrations on the ground. The method incorporates the directional sensitivity of rectangular detectors, the errors in the airborne data, and a source (forward) model that incorporates the 3D topographic variations in the survey area. The method is a significant improvement on current methods, and gives superior interpolation between flight lines. It also eliminates terrain effects that would normally remain in the data with the use of conventional gridding methods.

Note that Schwarz et al. (1992) published a method for correcting airborne gamma-ray spectrometric line data for terrain effects. While the method is not routinely used, it can significantly reduce terrain effects in areas of rugged topography. The correction is applied on a point-by-point basis to the line data before the height correction. The correction is a scaling of the data by a factor that is the ratio between the counts that would be observed at the observation point (for unit concentration of the radioelement) over a 3D topography, with that over a flat-earth topography at the observation height. The method is based on the assumption that, for each observation point, there is a uniform concentration of the radioelements within the field of view of the spectrometer. An example of the application of this method will be shown later in this paper.

The inversion model

The new method uses a source model comprising vertical rectangular prisms of uniform radioactivity and with the same horizontal dimensions as the required grid cell size. The top of each prism is a plane surface derived from a best-fit plane to the digital elevation model of the earth's surface within each grid cell area.

We start with the two-dimensional gamma-ray response, $f(x,y)$, of an elementary rod terminating at the earth's surface, adapted from the one-dimensional response given by Kogan et al. (1971) and Tammenmaa et al. (1976) as follows:

$$f(x,y) = \frac{Bh\exp(-\mu\sqrt{h^2 + r^2})}{(h^2 + r^2)^{3/2}} \qquad (1)$$

where $r = \sqrt{x^2 + y^2}$, x and y are the lateral distances from the source, μ is the linear attenuation coefficient of gamma rays in air for a particular energy, h is the height of the detector above the ground, and B is a constant that depends on the radioactivity of the rod, the energy of the radiation, and the sensitivity of the detector. We calculate the 2D response due to a vertical rectangular prism by integrating Equation 1 over the horizontal x and y dimensions of the prism. The response is then corrected for the directional sensitivity of the detector using the experimental relationship (Grasty, 1975; Tewari and Raghuwanshi, 1987)

$$A\varepsilon = A_0\varepsilon_0(a + b\cos\theta), \qquad (2)$$

where $A_0\varepsilon_0$ is the value of a collimated beam of gamma rays and θ is the angle between the vertical and the line from the source to the detector. The values a and b are determined experimentally. Grasty originally performed this experiment for a 9×4 in (22.8×10.1 cm) cylindrical detector. Tewari and Raghuwanshi repeated the experiment using the $16 \times 4 \times 4$ in ($40.6 \times 10.2 \times 10.2$ cm) slab detectors commonly used today. Billings et al. (2003) used a more rigorous procedure, based on first principles, to estimate the effect of detector geometry on sensitivity. Since the differences between the two methods are small, we have used the model and coefficients of Tewari and Raghuwanshi, for simplicity. We also correct the detector response for the velocity of the detector (Billings and Hovgaard, 1999).

The source-detector response for three different grid cell sizes (and hence prism sizes) is shown in Figure 1 for a 60 m flying height. The response will be narrower for lower flying heights. This shows that the response due to a rectangular prism extends well beyond the source, and its effects are measureable on several airborne samples (usually spaced either 30 m or 60 m along lines), as well as on at least one adjacent line on either side of the cell.

The inversion model is parameterised by considering, for any particular observation point (taken as the mid-point of the sample accumulation interval along the ground), all prisms that are within the field of view of the detector. This is typically prisms within a circle of radius of about five times the flying height, as the effect of radioactive prisms further away than this will have negligible effect at the observation point. We incorporate the topography into the model by replacing the top of each prism with a plane surface derived from a best-fit plane to the digital elevation model of the earth's surface within each grid cell area (Figure 2). The grid cell size is typically chosen as one-quarter of the flight line spacing. The geometry is shown in 2D section in Figure 3, where P is the observation point, and ABCD is the prism with a tilted top surface. The observation point is at a height h above ground level. With reference to Figure 3, the gamma-ray response due to the prism model is calculated as follows:

- We rotate the ground surface G_1 into the plane of the prism surface G_2 to calculate the response due to the vertical rectangular prism RSTU using Equations 1 and 2 at a height H above the hypothetical new ground level G_2.
- We then scale this response in proportion to the area of the top of prism ABCD to that of prism RSTU.

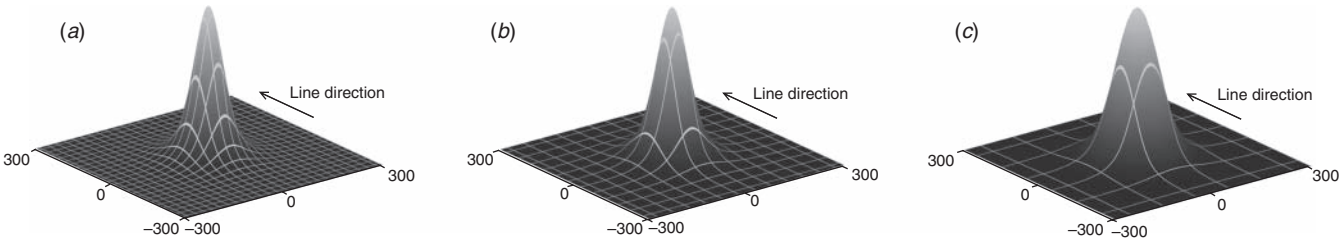

Fig. 1. Source-detector response for a slab detector (four $16 \times 4 \times 4$ in detectors laid side-by-side) at 60 m height above a vertical rectangular prism source centred at (0,0) with dimensions: (*a*) 25 m (top), (*b*) 50 m (middle), and (*c*) 100 m (bottom). The figures are 600 m wide in the x and y dimensions.

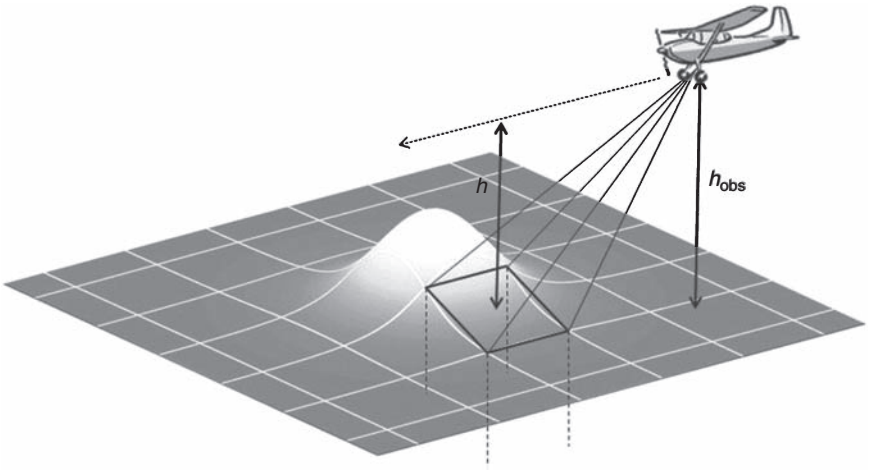

Fig. 2. Schematic showing the parameterisation of the topography using prism sources with slanted top surfaces relative to the detector.

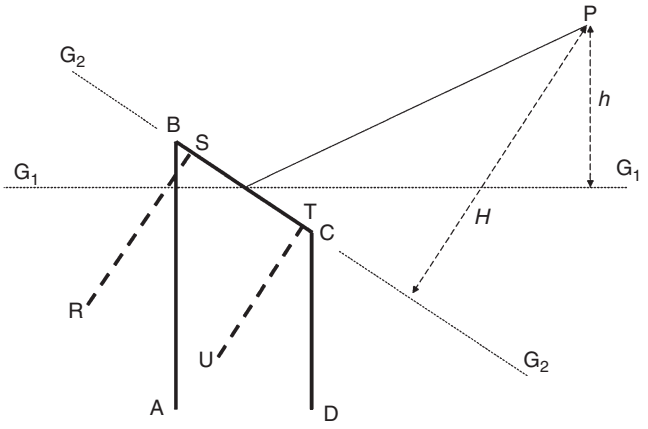

Fig. 3. 2D representation of the source-detector geometry (see text).

We use this approximation as there is no simple direct means of calculating the gamma-ray response due to a uniformly radioactive prism with a tilted top surface. Obviously, if the observation point P is above the plane surface BC, then the prism is visible at the detector. If the point P lies below the plane, then the prism is not visible at the detector, and its contribution to the observed radiation at P is zero. We also make the assumption that if the observation point P is above the plane surface BC, but the plane is either not visible, or only partially visible due to intervening topography, then the plane is still treated as visible. The errors introduced by this latter assumption are likely to be small, as any such planes are probably a considerable distance from the detector.

The inversion problem can now be explicitly stated as follows. Given N observations (and their associated errors) along the airborne survey flight lines, we wish to estimate the concentrations of M radioactive prisms that best predict the observed count rates at airborne height. The number of unknowns, M, is typically a factor of five times larger than the number of data, N. The problem can therefore only be solved by introducing regularisation to constrain smoothness into the inversion.

Inversion methodology

Using the terminology of Brodie and Sambridge (2006), we wish to minimise an objective function of the form

$$\Phi = \Phi_d + \lambda \Phi_m \tag{3}$$

where Φ_d is a data misfit term, and Φ_m is a model roughness term. The regularisation factor λ weights the relative importance of the data misfit and model roughness terms. The data misfit is defined as the weighted L_2 norm

$$\Phi_d = [\mathbf{Gm} - \mathbf{d}]^T \mathbf{C}_d^{-1} [\mathbf{Gm} - \mathbf{d}] \tag{4}$$

where $\mathbf{d}$ are the observed data (elemental count rates at airborne heights), and $\mathbf{m}$ are the unknown model parameters (concentration estimates for each prism). $\mathbf{G}$ is the sensitivity matrix whose entries, G_{ij}, are the contribution of the jth model prism to the ith datum for unit concentration of the radioelement in the prisms. Thus $\mathbf{Gm}$ is the forward model function that predicts the data based on the estimated model parameters. $\mathbf{C}_d$ is the data covariance matrix. For gamma-ray spectrometric data, there is no covariance between datum errors as each measurement occurs independently of every other, so $\mathbf{C}_d^{-1}$ is a diagonal matrix with elements $1/v$, where v is the variance of each datum. How these errors are estimated is discussed later in this section.

The model roughness term is defined as

$$\Phi_m = \mathbf{m}^T \mathbf{L}^T \mathbf{L}\mathbf{m} \tag{5}$$

where $\mathbf{L}$ is the second finite difference roughness operator (..1–2 1..), which is applied in both E–W and N–S directions.

The objective function

$$\Phi = \Phi_d + \lambda \Phi_m = [\mathbf{Gm} - \mathbf{d}]^T \mathbf{C}_d^{-1} [\mathbf{Gm} - \mathbf{d}] + \lambda \mathbf{m}^T \mathbf{L}^T \mathbf{L}\mathbf{m} \tag{6}$$

is minimised when its derivative with respect to the model parameters $\mathbf{m}$ is zero; that is, when

$$\frac{\partial \Phi}{\partial \mathrm{m}} = 2\mathbf{G}^T \mathbf{C}_d^{-1} [\mathbf{Gm} - \mathbf{d}] + 2\lambda \mathbf{L}^T \mathbf{L}\mathbf{m} = 0. \tag{7}$$

After cancelling the $2s$ and collecting $\mathbf{m}$ on the left-hand side we get the linear system to be solved:

$$[\mathbf{G}^T \mathbf{C}_d^{-1} \mathbf{G} + \lambda \mathbf{L}^T \mathbf{L}]\mathbf{m} = \mathbf{G}^T \mathbf{C}_d^{-1} \mathbf{d} \tag{8}$$

Note that the regularisation matrix $\mathbf{L}^T\mathbf{L}$ is extremely sparse (Li and Oldenburg, 2010; Menke, 1989). The sensitivity matrix $\mathbf{G}$ is also sparse, as the gamma-ray response can be considered as effectively zero for distances greater than ~500 m from the source. The exact cut-off distance is a function of the energy of the

radiation, and the height of the detector above the ground. To invert our airborne data to a grid of elemental concentrations we solve the linear system (Equation 8) using the preconditioned conjugate gradient method implemented via the open-source PETSc code (Balay et al., 2014).

Estimating the errors in the input data

The accurate estimation of the errors in the input data is essential for the successful solution of most geophysical inverse problems. Not only do we use the errors to appropriately weight the input data, but the errors also gives us a measure to ensure that our preferred model does not over-fit the data. For example, we may want our preferred model to fit our observation to just within the noise envelope, but no more – as we don't want to be fitting the noise. This is particularly important for gamma-ray spectrometric data where errors are large.

Most of the noise in observed gamma-ray spectra derives from the statistical nature of radioactive decay. Each radioactive decay is a random event. But if we average the number of decays (and subsequently recorded gamma rays) over a large sampling period, then the concentration of the radioactive isotope is proportional to the mean count rate. The statistical counting errors in gamma-ray spectrometry follow a Poisson distribution, and a special property of this distribution is that the variance is equal to the mean. So if we assume that all of the errors are due to the random nature of radioactive decay, and if we can estimate the mean count for a gamma-ray measurement, then we have an estimate of the variance of that measurement.

We estimate the errors in each observed gamma-ray spectrum using the associated noise-reduced spectrum, derived using either the noise-adjusted singular value decomposition (NASVD) (Hovgaard, 1997; Hovgaard and Grasty, 1997) or minimum noise fraction (MNF) (Green et al., 1988; Dickson and Taylor, 1998; Lee et al.,1990) methods, as our estimate of the mean spectrum, and hence variance for each channel. Figure 4 shows a typical 1-s airborne gamma-ray spectrum recorded at 60 m height with a 32 L NaI detector. The noise-reduced NASVD spectrum and the positions of the conventional K, U and Th windows are also shown. The noise-reduced spectrum gives a good estimate of the mean spectrum, and hence variance for each channel count rate. While some noise is still evident in the NASVD spectrum, these errors will be effectively further averaged through summing over the conventional 3-channel K, U and Th windows in the first step of the data processing procedure.

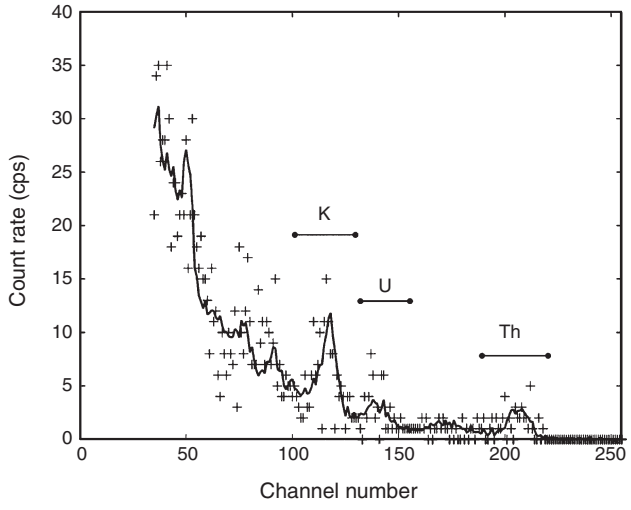

Fig. 4. Typical 1-s airborne gamma-ray spectrum recorded at 60 m height with a 32 L NaI detector (crosses). The noise-reduced NASVD spectrum (solid line), and the positions of the conventional K, U and Th windows are shown.

The errors in noise-reduced NASVD or MNF 3-channel data are estimated using a slightly different approach. We generate 3-channel data using both the raw spectra and the noise-reduced spectra. These 3-channel data (K, U and Th window count rates along the flight lines) are low-pass filtered using the filter described by Tammenmaa et al. (1976). We then use the differences between the filtered and unfiltered profiles as a measure of the errors in both the raw 3-channel data and the noise-reduced data in order to calculate the fractional reduction in errors (for each of K, U and Th) achieved by NASVD or MNF. These fractional reductions are applied to the estimated errors in the raw 3-channel data, which are then used as estimates of the errors in the noise-reduced data.

We recognise that while the above procedure for estimating the errors may not be entirely accurate, we feel that it is better to have a rough approximation of the errors for the purpose of weighting the data in the inversion, rather than no error weighting at all.

Let us assume that the estimated errors are uncorrelated, random, and normally distributed. For a function of two variables, $f(x,y)$, with known standard deviations (σ_x and σ_y, say) associated with the variables x and y, the standard deviation in $f(x,y)$ is given by:

$$\sigma_f = \sqrt{\left(\frac{\partial f}{\partial x}\right)^2 (\sigma_x)^2 + \left(\frac{\partial f}{\partial y}\right)^2 (\sigma_y)^2} \qquad (9)$$

We use Equation 9 to propagate the raw 3-channel count rate errors through the data processing procedures to get estimates of the errors in the final radioelement estimates.

The errors in radioelement estimates derived from airborne gamma-ray spectrometric data are generally high. Fractional standard deviations of around 8–12% for K and eTh, and over 30% for eU are typical. Of greater interest is that errors can vary considerable from line to line, depending on prevailing background radon concentrations and the height of the detector. Minty et al. (1997) demonstrated how high radon levels, or large height deviations, can have significant effects on the errors in the final radioelement estimates. For example, the height-correction required to adjust U channel data acquired at 250 m height to a nominal survey height of 80 m requires the data to be scaled up by a factor of 7. The errors in the data scale by the same amount. An example is given later in this paper.

Practical considerations

There are two issues that require consideration for the practical implementation of the method:

- The method is applied to airborne gamma-ray spectrometric line data after the data have been background-corrected and stripped. That is, the inversion incorporates (replaces) the height and sensitivity corrections. It converts the K, U and Th elemental count rates, measured at each observation height, to grids of elemental concentrations on the ground. This raises the issue of levelling errors in the data – artefacts introduced through inadequate background removal. If present, these are normally removed after the height and stripping corrections using crossover tie levelling and microlevelling. We overcome this problem by using as our starting point the fully-processed, level data. We then 'undo' the sensitivity and height corrections before inverting the data. This assumes that the levelling procedures (if applied) have not removed any artefacts relating to topography. This is a reasonable

assumption as levelling corrections are always limited to long-wavelength features in the line direction.

- The method requires that we know the sensitivity of the detector to a prism source over a range of heights and lateral distances from the observation point. But the constant B in Equation 1, which incorporates the detector sensitivity, is unknown. We 'calibrate' our response functions by ensuring that (a) the sum of the responses of all prisms within the field of view of the detector (which is effectively the broad-source response) at the nominal survey height is consistent with the measured broad-source sensitivities acquired from the conventional sensitivity calibration, and (b) ensuring that the sum of the responses of all prisms at any other height is consistent with the broad source response at the nominal survey height, bearing in mind that we know from our height-attenuation coefficient calibrations how the broad-source response changes with deviations from the nominal survey height.

Application to airborne data

We use two metrics to guide our choice of regularisation parameter for the application of the inversion method to real airborne data – the data misfit (Equation 4), and the model roughness (Equation 5). If we repeat the inversion for a complete range of values of the regularisation parameter λ, we get the typical 'L' curve (Hansen, 1997) shown in Figure 5. At the corner of the L-curve a change in λ produces approximately equal changes in both the data misfit and model roughness, and can be considered as the value that produces a good balance between data misfit and model roughness (Farquharson and Oldenburg, 2004). Alternatively, we can use our knowledge of the errors in the data to guide our choice of λ. For example, we could choose a value of λ that fits the data to just within the noise envelope. But in practice, we find that if we do this the resulting grid tends to be quite smooth – particularly for U where the errors are large. We prefer to use the minimum curvature grids as a guide, and choose a value of λ by trial and error that sharpens up anomalous features while still smoothing at least some of the noise.

Figure 6 shows an example from the Fowler's Gap survey, New South Wales, flown at a nominal height above ground level of 60 m. The terrain height changes by over 200 m across this area. The 'herringbone' pattern in the aircraft height

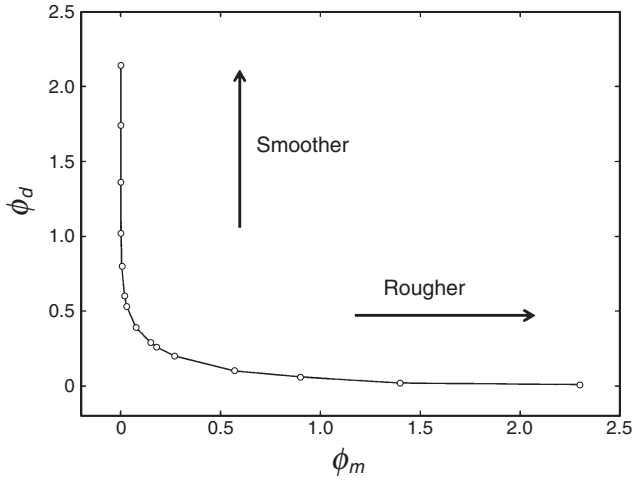

Fig. 5. Potassium 'L-curve' for a portion of the Fowler's Gap survey. The value of λ tends to infinity for large φ_d and to zero for large φ_m. The point $\varphi_d = 1$ corresponds to the value of λ where the model fits the data to the estimated noise level.

(Figure 6*a*) is a result of the aircraft performance requiring a gradual climb to clear the mountain in one direction, and a rapid descent in the other direction. Height differences on adjacent lines are up to 100 m. These translate into difference in error variance on adjacent lines up to a factor of 3 (Figure 6*b*). This demonstrates the importance of weighting the data according to their variances. The 3D inversion gives far greater weight to those line data acquired closer to the ground. Figure 6*c* shows K concentrations gridded using minimum curvature, and Figure 6*d* shows the 3D inversion where the model fits the data to just within the level of the noise, but no further ($\Phi_d = 1$ in Figure 5). This gives a relatively smooth result with good definition of the K variation.

Figure 7 shows an example from the South-East Lachlan survey, New South Wales. The survey was flown at 60 m height over an area that is quite mountainous in parts. Figure 7*a* shows the digital elevation model over part of the survey area, which shows elevation changes of up to 900 m. The inability of the fixed-wing aircraft to fly a drape surface has resulted in large deviations from the nominal survey height, which then propagates as errors into the final radioelement estimates. In some places the aircraft was more than 400 m above ground level. The K concentration variances are shown in Figure 7*b* and vary in places by more than a factor of 20.

The minimum curvature grid is shown in Figure 7*c* and the 3D inversion equivalent in Figure 7*d*. The 3D inversion grid is a significant improvement on the minimum curvature grid as follows:

- The 3D grid shows better continuity of anomalous features and better interpolation between flight lines. The positions of the flight lines are evident in the minimum curvature grid as E–W lines of high-frequency speckle corresponding to the original observation points.
- The 3D gridding has a natural tendency to smooth the grid in areas where the error variances are large. This is a logical consequence of the data being given less weight, relative to the smoothing term in Equation 8, as the errors in the data increase. This is an improvement on the minimum curvature grid which tends to grid noise in these areas.
- The incorporation of the topography into the inversion can be clearly seen at several places. In the deeply-weathered Australian environment the tops of mountains and ridges, which are actively eroding and thus exposing fresh rocks and soils, often show higher K concentrations than other more deeply-weathered parts of the landscape (Wilford et al., 1997). As the aircraft passes over a ridge, many of the sources within the field of view are further from the detector than is the case for a flat earth. In these circumstances conventional methods underestimate radioelement concentrations as the data are corrected for the height of the ground directly beneath the aircraft assuming flat-earth geometry. The opposite is true over valleys, where conventional methods tend to overestimate the concentrations directly beneath the aircraft. This effect is evident along the ridges in Figure 7 – we speculate that the 3D inversion is correctly identifying the increase in K concentration whereas the conventional processing is not.

A second example from the South-East Lachlan survey is shown in Figure 8. Figure 8*c* shows the topographic correction factors of Schwarz et al. (1992). This is a scaling factor which scales the data up over the tops of ridges where the earth is concave downward, and down over valleys and gorges where the earth is concave upward. The 'topographically-corrected' K concentrations are shown in Figure 8*d*. Using the final conventionally-processed data as a starting point, these were

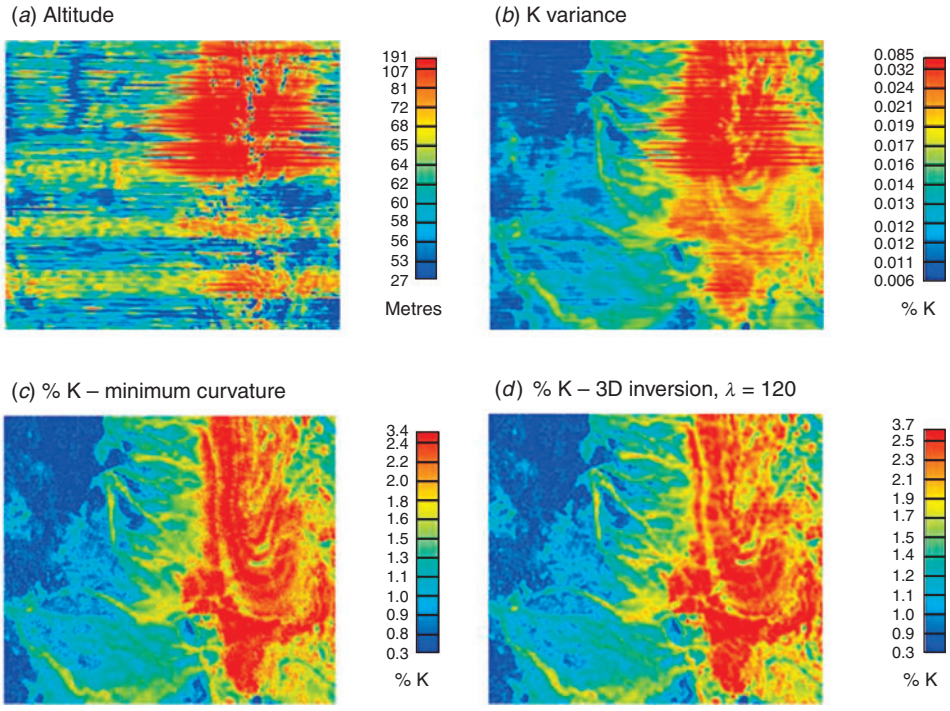

Fig. 6. Pseudo-colour images from the Fowler's Gap survey area: (*a*) detector height above ground level, (*b*) K concentration variance, (*c*) K concentration (%) gridded using minimum curvature, and (*d*) K concentration gridded using 3D inversion so as to not fit the noise. The images are centred on (141 : 22 : 59.10 E, 31 : 05 : 38.86 S) and are ~22 km wide. Data courtesy of Geoscience Australia.

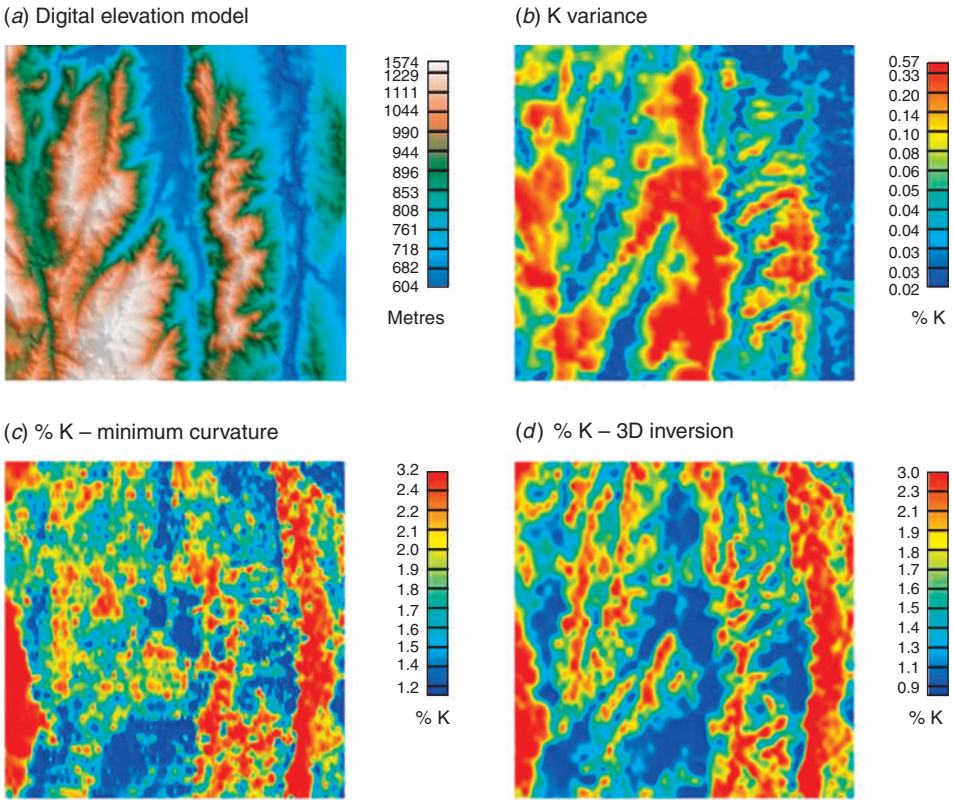

Fig. 7. Pseudo-colour images from the South-East Lachlan survey area: (*a*) digital elevation model, (*b*) K concentration variance, (*c*) K concentration (%) gridded using minimum curvature, and (*d*) K concentration gridded using 3D inversion so as to not fit the noise. The images are centred on (149 : 04 : 39.99 E, 35 : 40 : 25.74 S) and are ~15 km wide. Data courtesy of the Geological Survey of New South Wales.

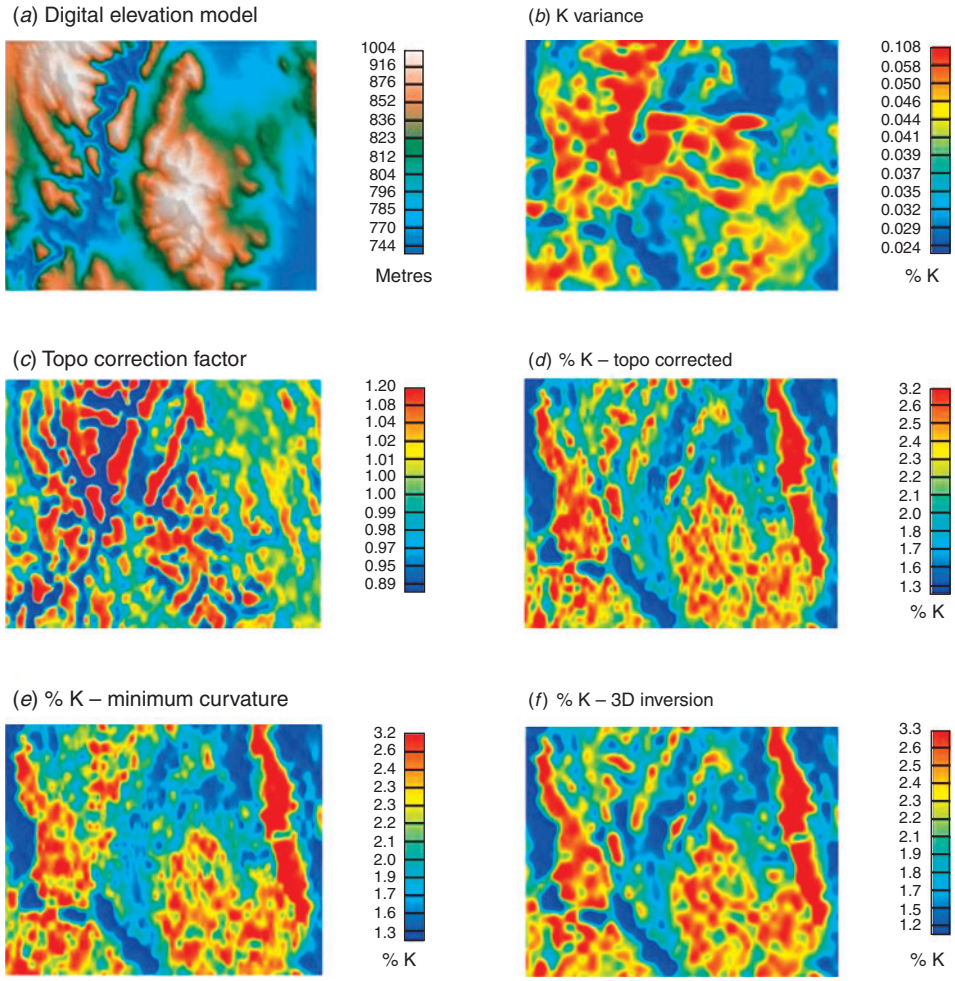

Fig. 8. Pseudo-colour images from the South-East Lachlan survey area: (*a*) digital elevation model, (*b*) K concentration variance, (*c*) topographic correction factor (see Schwarz et al. (1992)), (*d*) K concentration (%) topographically-corrected using the method of Schwarz et al. (1992), (*e*) K concentration (%) gridded using minimum curvature, and (*f*) K concentration gridded using 3D inversion. The images are centred on (149.1 E, 36.1 S) and are ~7.8 km wide. Data courtesy of the Geological Survey of New South Wales.

derived by: 'undoing' the sensitivity and height corrections; applying the topographic correction scaling factors; then redoing the height and sensitivity corrections. The minimum curvature and 3D inversion grids are shown in Figure 8*e*, *f* for comparison. In spite of the fact that the method of Schwarz et al. is based on the assumption that the concentration of radioelements in the earth are uniform within the field of view of the spectrometer, the results are similar to that of the 3D inversion. The 3D inversion grid is obviously smoother (as the inversion result is constrained to be smooth), but also results in better feature definition through improved interpolation between flight lines.

Note that there is no practical limit to the size of surveys that can be processed using the new methodology as the survey area can be split into overlapping tiles for processing. The method is thus also amenable to parallelisation to speed up the computations. For example, a single inversion for the South-East Lachlan survey (107000 km at 250 m line spacing) completes in under 30 minutes using an Intel Core I7 Extreme 990X CPU (six cores).

Conclusion

The new method is more than just a gridding technique. It is a physics-based method for the rigorous inversion of airborne gamma-ray spectrometric line data to elemental concentrations on the ground. The method incorporates the height of the aircraft, the 3D terrain within the field of view of the spectrometer, and the directional sensitivity of the rectangular detectors currently used in airborne surveying. The resulting grids of elemental concentrations are a significant improvement on those derived using conventional methods. The 3D inversion gives better interpolation between flight lines, and incorporates our knowledge of errors in the data into the final grid. It also eliminates terrain effects that would normally remain in the data with the use of conventional processing methods.

Acknowledgements

We thank an anonymous referee for insightful comments that have significantly improved this paper. One of the authors (RB) publishes with the permission of the CEO, Geoscience Australia.

References

Balay, S., Abhyankar, S., Adams, M. N. F., Brown, J., Brune, P., Buschelman, K., Eijkhout, V., Gropp, W. D., Kaushik, D., Knepley, M. G., McInnes, L. C., Rupp, K., Smith, B. F., and Zhang, H., 2014, PETSc web page. Available at http://www.mcs.anl.gov/petsc

Billings, S., and Hovgaard, J., 1999, Modeling detector response in airborne gamma-ray spectrometry: *Geophysics*, **64**, 1378–1392. doi:10.1190/1.1444643

Billings, S. D., Minty, B. R. S., and Newsam, G. N., 2003, Deconvolution and spatial resolution of airborne gamma-ray surveys: *Geophysics*, **68**, 1257–1266. doi:10.1190/1.1598118

Brodie, R., and Sambridge, M., 2006, A holistic approach to inversion of frequency domain airborne EM data: *Geophysics*, **71**, G301–G312. doi:10.1190/1.2356112

Craig, M., Dickson, B., and Rodrigues, S., 1999, Correcting aerial gamma-ray survey data for aircraft altitude: *Exploration Geophysics*, **30**, 161–166. doi:10.1071/EG999161

Dickson, B., and Taylor, G., 1998, Noise reduction on aerial gamma-ray surveys: *Exploration Geophysics*, **29**, 324–329. doi:10.1071/EG998324

Druker, E., 2012, Processing of aero gamma-ray spectrometry data as 2D inverse problem: 22nd International Geophysical Conference and Exhibition, 26–29 February 2012, Brisbane, Australia, 1–4.

Farquharson, C. G., and Oldenburg, D. W., 2004, A comparison of automatic techniques for estimating the regularization parameter in non-linear inverse problems: *Geophysical Journal International*, **156**, 411–425. doi:10.1111/j.1365-246X.2004.02190.x

Grasty, R. L., 1975, Atmospheric absorption of 2.62 MeV gamma-ray photons emitted from the ground: *Geophysics*, **40**, 1058–1065. doi:10.1190/1.1440582

Green, A. A., Berman, M., Switzer, P., and Craig, M. D., 1988, A transformation for ordering multispectral data in terms of image quality with implications for noise removal: *IEEE Transactions on Geoscience and Remote Sensing*, **26**, 65–74. doi:10.1109/36.3001

Gunn, P. J., 1978, Inversion of airborne radiometric data: *Geophysics*, **43**, 133–143. doi:10.1190/1.1440816

Hansen, P. C., 1997, *Rank-deficient and discrete ill-posed problems: numerical aspects of linear inversion*: SIAM.

Hovgaard, J., 1997, A new processing technique for airborne gamma-ray spectrometer data (noise adjusted singular value decomposition): *American Nuclear Society Sixth Topical Meeting on Emergency Preparedness and Response*, San Francisco, 22–25 April 1997, 123–127.

Hovgaard, J., and Grasty, R. L., 1997, Reducing statistical noise in airborne gamma-ray data through spectral component analysis, *in* E. G. Gubins, ed., *Proceedings of Exploration 97: Fourth Decennial Conference on Mineral Exploration*: Prospectors and Developers Association, 753–764.

IAEA, 2003, Guidelines for radioelement mapping using gamma-ray spectrometry data: IAEA-TECDOC-1363, International Atomic Energy Agency, Vienna.

Kogan, R. M., Nazarov, I. M., and Fridman, Sh. D., 1971, *Gamma spectrometry of natural environments and formations*. Translated 1971 by Israel Program for Scientific Translations Ltd. No. 5778, available from the US Department of Commerce, National Technical Information Service, Springfield, VA, 22151, 337 pp.

Lee, J. B., Woodyatt, A. S., and Berman, M., 1990, Enhancement of high spectral resolution remote-sensing data by a noise-adjusted principal components transform: *IEEE Transactions on Geoscience and Remote Sensing*, **28**, 295–304. doi:10.1109/36.54356

Li, Y., and Oldenburg, W., 2010, Rapid construction of equivalent sources using wavelets: *Geophysics*, **75**, L51–L59. doi:10.1190/1.3378764

Menke, W., 1989, *Geophysical data analysis: discrete inverse theory*: Academic Press.

Minty, B. R. S., Luyendyk, A. P. J., and Brodie, R. C., 1997, Calibration and data processing for airborne gamma-ray spectrometry: *AGSO Journal of Australian Geology & Geophysics*, **17**, 51–62.

Schwarz, G. F., Klingele, E. E., and Rybach, L., 1992, How to handle rugged topography in airborne gamma-ray spectrometry surveys: *First Break*, **10**, 11–17.

Tammenmaa, J. K., Grasty, R. L., and Peltaniemi, M., 1976, The reduction of statistical noise in airborne radiometric data: *Canadian Journal of Earth Sciences*, **13**, 1351–1357. doi:10.1139/e76-140

Tewari, S. G., and Raghuwanshi, S. S., 1987, Some problems on the range of investigation in airborne gamma-ray spectrometry: *Uranium*, **4**, 67–82.

Wilford, J. R., Bierwirth, P. N., and Craig, M. A., 1997, Application of airborne gamma-ray spectrometry in soil/regolith mapping and applied geomorphology: *AGSO Journal of Australian Geology & Geophysics*, **17**, 201–217.